PASSIVE DETECTOR TECHNOLOGY FOR THE CAPTURE OF MICROMETEOROIDS AND ORBITAL DEBRIS: CALORIMETRIC AEROGELS

G. Dominguez[(1)], A.J. Westphal[(1)], M.L.F Phillips[(2)] , S.M. Jones[(3)], G.A. Graham[(4)], A.T. Kearsley[(5)] and G. Drolshagen[(6)]

[(1)]Space Sciences Laboratory, University of California at Berkeley, CA, USA, domi@socrates.berkeley.edu
[(2)]Pleasanton Ridge Research Corporation, Hayward, CA, USA
[(3)]Jet Propulsion Laboratory, California Institute of Technology, Pasadena, CA, USA
[(4)]IGPP, Lawrence Livermore National Laboratory, Livermore, CA, USA
[(5)]Department of Mineralogy, The Natural History Museum, London, UK
[(6)]ESTEC, European Space Agency, Noordwijk, NL

ABSTRACT

The post-flight investigations of retrieved surfaces previously exposed in low-Earth orbit (LEO) allow an insight into the micro-particle environment (both orbital debris and micrometeoroids) that maybe hazardous to operational orbiting spacecraft. However, such investigations are typically periodic and opportunistic. Furthermore, the retrieved materials are rarely optimized in construction for the capture and preservation of micrometeoroids and orbital debris. Therefore particle remnants are observed as complex residues that are highly altered from their original state and intimately associated with the impacted surface surface (e.g. Graham et al., 2004). As a result, determination of origin of the residues is generally highly subjective and inconclusive.

The scientific and technical requirements for current and future sample return missions to small bodies have resulted in the use of low-density materials (Maag and Linder, 1992). Silica aerogels have proved to be a highly effective capture cell technology to enable the recovery of particulate material after hypervelocity encounters (e.g. Tsou et al., 1990 and Barrett et al. 1992). Silica aerogels have been deployed successfully on both the Mir space station and the International Space Station (ISS) to capture micro-particles in LEO (Hörz et al., 2000 and Kitazawa et al., 2000). As passive detectors, aerogel have enabled detailed studies of particle both micrometeoroid and orbital debris in terms of chemical composition (Hörz et al., 2000). However it can be time consuming to distinguish micrometeoroids and orbital debris impact tracks other than performing detailed chemical characterization that may require extraction (Westphal et al. 2002; 2004) or access to sophisticated instrumentation to enable *in-situ* measurements (e.g. Borg et al., 2004) Furthermore there is no quantitative indication of impact velocity. Both velocity information and rapid discrimination of particle origin are highly desirable for any passive detector to be flown on the European proposed Standardized Container for Experiments (SCE) on ISS to monitor LEO environment (Kearsley et al. this volume).

We have developed a so-called "calorimetric" aerogel that may be used to capture, locate, and measure the velocities of grains in low earth orbit. The heat pulse caused by the capture of a hypervelocity grain in this aerogel induces a permanent, local phase transformation to a crystalline phase with dramatically enhanced fluorescence compared to the unheated amorphous phase. The capture of a hypervelocity grain is marked by a unique signature --- a fluorescent spot that is easily visible under a low-power fluorescence microscope. More importantly, we have demonstrated experimentally that this aerogel acts as a calorimeter, capable of passively measuring grain kinetic energy. Thus, a simple estimate of the captured mass, together with the fluorescent signal, allows one to make a quantitative measurement of the impact velocity.

Calorimetric aerogel is a significant advance in passive detector technology as it enables both chemical and physical measurements to be carried out on the captured particles while simultaneously giving information about their velocities.

1. INTRODUCTION

Aerogels have the lowest densities of any solids known. Unlike organic foams, which can be made with somewhat comparable densities, aerogels are porous at the submicron scale. The combination of low density and nano-porosity enables aerogels to capture a wide range of hypervelocity projectile sizes relatively intact (Burchell et al., 1999).

A large aerogel collector (ODC) has previously been deployed in low-Earth orbit, but a severe background of anthropogenic orbital debris has so far prevented the identification of more than a handful of natural micrometeorites (Hörz et al., 2000). No interstellar particles have been identified so far. Since they are on hyperbolic orbits, interstellar and interplanetary dust

grains are faster than orbital debris, so could in principle be identified on the basis of their impact velocities.

Unfortunately, conventional SiO_2-based aerogels provide little information on impact velocity of a captured dust grain. The capture of a hypervelocity dust particle in aerogel produces a shock wave that deforms, heats, and vaporizes the aerogel material in the vicinity of the projectile's trajectory, resulting in the formation of a permanent track or impact cavity. The experimentally observed correlation between captured projectile velocity and track characteristics (e.g., track length, track radius, etc.) is poor (Kitazawa, 1999). These poor correlations are also expected theoretically (Anderson and Ahrens, 1994; Domínguez et al., 2004). Therefore, natural micrometeorites captured in the ODC collector have only been identified after time-consuming chemical analysis.

1.1. Calorimetric Aerogels

We developed calorimetric aerogels as a means of capturing and distinguishing between the low-velocity orbital debris "background" and the higher velocity extraterrestrial (interstellar and interplanetary) dust grains that would be captured in LEO. They work as follows: the capture and deceleration of a hypervelocity projectile deposits heat along its trajectory inside the aerogel. In previous work, we have demonstrated that hypervelocity projectiles captured in Gd,Tb-doped Al_2O_3 aerogels produce tracks that fluoresce under ultraviolet light (See Fig. 1) (Domínguez et al., 2003). In addition, we have shown that the amount of fluorescence produced by an impact cavity is an increasing function of the kinetic energy of the projectile, with a response function of the form:

$$S \propto E^n \qquad (1)$$

where n~2/3.

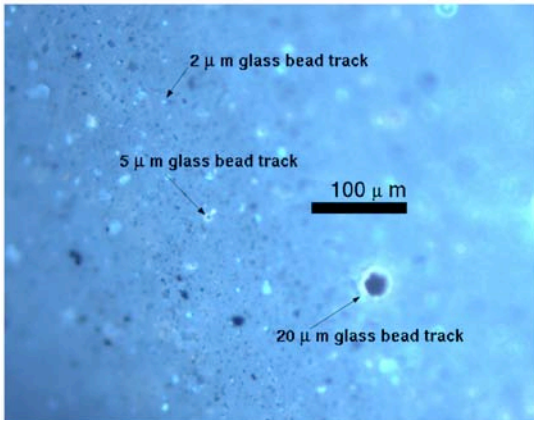

Figure 1. Fluorescent tracks of 2,5, and 20 micron sized glass beads impacts at v=3.2 km/s. The image was taken at 10x magnification and integrated for 7 seconds.

Our first samples of calorimetric aerogels were not monolithic, consisting of pieces with dimensions typically on the order of 1 mm and with densities on the order of about 180 mg/cc. By comparison, the Stardust aerogels have densities on the order of 20 mg/cc.

The techniques for making Al_2O_3 aerogels are not as refined as those used for making SiO_2 aerogels. In order to have a sample of aerogel that was suitable for spaceflight, we looked for additional aerogel compositions that can be used as calorimetric aerogels. Since 2002, we have been working on developing a monolithic, calorimetric aerogel that is sensitive to small (~1 micron) projectiles. As part of this development work, we have been synthesizing and testing a variety of aerogels with various matrix (e.g. SiO_2, Al_2O_3, SiO_2-Al_2O_3, etc.) and dopant compositions (Gd:Tb, Zn, Ti, Er:Yb, etc.) in search of an aerogel with optimal mechanical and calorimetric properties.

In this paper, we present preliminary results on the response function and velocity resolution of a flight-ready sample of calorimetric aerogel that was recently discovered.

2. METHODS

2.1. Aerogel Synthesis

The monolithic, calorimetric aerogel, which we call 186-2, was made using standard aerogel synthesis techniques for making SiO_2 aerogels and doped with Gd and Tb.

The silica sol was prepared (by M.L.F.P.) using a method typical of that described in Hrubesh et al., 1992. First, a mixture of 114 g TEOS (Aldrich, 99.9%), 114 g absolute ethanol (Aaper), 6.00 g H_2O, and 4.0 g 0.1 N HCl was stirred overnight at 50°C. Ethanol was distilled off under vacuum in a rotary evaporator until the sol was noticeably viscous. 200 mL acetonitrile (HPLC grade, Fisher) was added and the sol was rotovaped (until the volume was reduced by approximately two-thirds. 200 additional mL CH_3CN was added and the process was repeated twice more. The final sol was diluted to a total volume of 300 mL with acetonitrile.

40 mL of this sol was added to 10.68 g $Gd(NO_3)_3 \bullet 6H_2O$ and 0.70 g $Tb(NO_3)_3 \bullet 5H_2O$ in a glass media bottle and stirred until dissolved. A mixture of 1.96 g H_2O and 5.94 g propylene oxide was added. The sol was agitated and poured into a stainless steel mold to gel. Gelation occurred after 2 days at room temperature.

The gel was covered with fresh acetonitrile and aged for 16 weeks prior to supercritical fluid extraction.

The acetonitrile fluid was extracted (by S.M.J.) as follows: The wet gel was placed onto a rack and immersed in reagent grade acetonitrile in the extraction vessel. After sealing the reaction vessel, the pressure was increased to roughly 775 psi with argon at a rate of roughly 25 psi/min. The vessel was leak checked first before ramping up the heat (~0.5^{o}C/min). This heating rate was maintained until the temperature reached about 260^{o}C, after which it was slowed to about 0.3^{o}C/min. The temperature ramp up was continued past 265-270^{o}C (where it became supercritical). The pressure during this time was monitored regulated at about 800 psi by releasing fluid from the vessel. When the temperature in the vessel reached 295^{o}C, this temperature is maintained and the vessel was gradually depressurized using an automated needle valve at a rate of 0.5 psi/min until an ambient pressure was reached. The gel and molds were allowed to cool overnight.

Upon manufacture, sample 186-2 had a brownish color, typical of doped aerogels that are prepared using the methods described above. This aerogel was mechanically robust (See Fig. 2) and fragments of this monolith were cut with a razor blade and placed in acrylic sample holders to prepare them for hypervelocity shot tests at NASA Ames Vertical Gun Range in Moffett Field, CA, U.S.A.

Figure 2. 186-2 SiO_2 aerogel monolith

2.2. Hypervelocity Shot Tests

During September 2004 and March 2005, individual portions of this sample were exposed to a mixture of 2, 5 and 20 micron sized (diameter) at v=2.05, 3.20, 4.05, 4.92, 5.41, and 5.91 km/s.

2.3. Fluorescence Imaging and Analysis

The fluorescence signal of individual impact tracks was measured using a standard fluorescence microscope at the Biological Imaging Facilities (BIF) at U. C. Berkeley with a cooled color (R,G,B channels) CCD camera. The fluorescence was excited at 360 nm and the excitation side and the emission was filtered with a long pass filter (λ>395 nm). The samples were imaged within 4 hours of each other to minimize the effects of UV lamp intensity variations. We acquired RGB images containing enough individual tracks to provide us with a statistically significant measurement of the response of each of the glass bead populations at each of the shot velocities.

For the analysis, we visually categorized the impact tracks from hypervelocity projectiles that entered the aerogel normal to its surface. This was straightforward to do for the 20 and 5 micron sized glass beads. The remaining impacts were classified as being the 2 micron glass bead population.

We quantified the amount of fluorescence from each track as follows:

1. a local region of the image was selected.
2. A local fluorescence background was taken from this region by selecting pixels in this box that were far removed from an impact track.
3. The background was subtracted from each of image that was proportional to the blue channel (since the background fluorescence was mostly in the blue).
4. A hot map consisting of those pixels whose value was 1σ above the noise was used to further restrict which pixels were associated with an individual impact (See Fig. 3.).
5. The signal was found by adding up the R+G+B pixel values of these regions

The signal, for an individual track consisted of adding up the pixel value of those pixels whose values of R+G+B was greater than 1σ above the background. This image analysis was done to ensure that only a change in the color (fluorescence) of the aerogel would produce a signal. In Fig. 4, we show a characteristic hot-map of an image of an impact of a 20 micron sized glass bead into the aerogel at impact and the pixels that contribute to the signal.

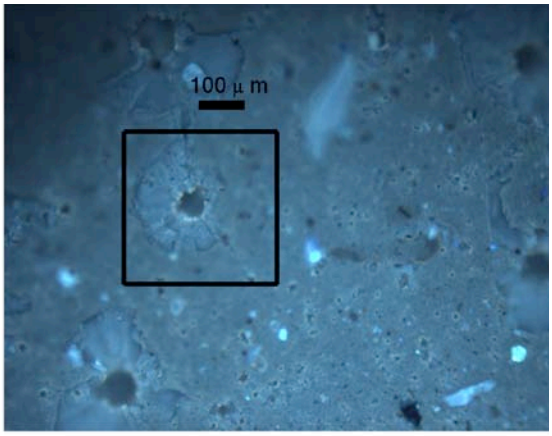

Figure 3. Fluorescence image of the surface of aerogel 186-2 shot with v=5.91 km/s particles. The box encapsulates the impact track of a captured 20 micron glass bead and several 5 micron glass bead impacts (See Fig. 4).

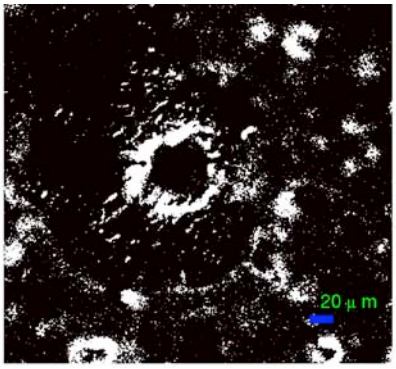

Figure 4. Background subtracted image showing pixels with values > 1σ above the noise. This region is part of the boxed in region in Fig.3.

3. RESULTS

3.1. Response Function

We have assumed that the response function of sample 186-2 has the form:

$$S = Ar^a v^b \qquad (2)$$

where A is a normalization constant and a and b are parameters that must be found iteratively. The normalization constant may depend on the density of the particles. Since we only shot glass beads, we are not sensitive to the relationship between A and the density. To find the best fit, we chose the normalization constant to lie in the geometric center of the 20 micron impact data (Q_{ref}, I_{ref}), where Q_{ref}=[min(S_{20})+max(S_{20})]/2, I_{ref}=[min(Q_{20})+max(Q_{20})], and the quantify $Q=r^a v^b$ for each of the populations. We found the best fit to the data by fixing the value of a, in the range [0.1-3] and finding the value of b that minimized the χ^2 statistic. The best combination for a and b to the 5 and 20 micron events was then chosen by visual inspection of the plotted data. We excluded the 2 micron glass bead impacts because we believe that these glass beads may have clumped together. It is also possible that since all of the impacts were chosen by eye, that the selection of fluorescent impact crater from this population are biased toward the larger members of this population. Fig. 6 shows the best fit line to these data. We have included the 2 micron data for reference.

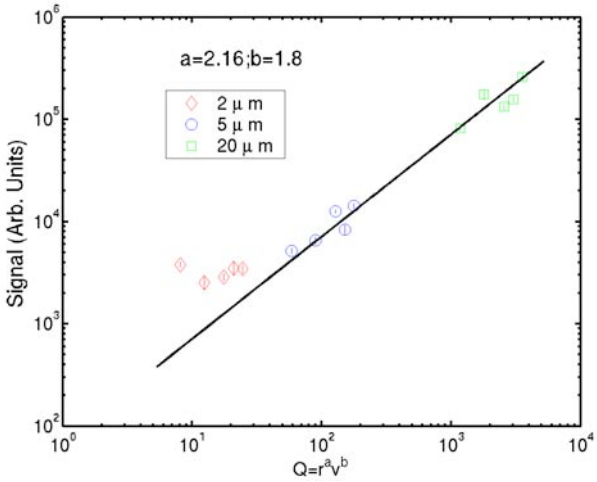

Figure 5. Response function of 5, and 20 micron sized populations. The values of a and b shown appear to be a good fit to the 5 and 20 micron glass bead populations. We have included the 2 micron population for reference.

3.2. Signal Dispersion

It is worth noting that deviation of the individual data points from the best line fit is larger than the error bars on the medians of each point. Thus, while there appear to be systematic effects that are contributing to the scatter we observe, the measurements of the response, for each dust size and velocity, are consistent enough to make an estimate of the velocity resolution of sample 186-2.

We assumed that response of the detector is a function of the velocity v, the projectile radius r and the projectile's density ρ. For a statistically large sample of identical impacts, small uncorrelated random deviations of the projectile's velocity, radius, and density (σ_v, σ_r, and σ_ρ) will produce a random distribution of the signal (σ_s). The detector will also contribute a noise term

(σ_{noise}) that adds in quadrature. Therefore, the square of the fractional dispersion in the observed signal (σ_S/S) can be expressed as:

$$\left(\frac{\sigma_S}{S}\right)^2 = \frac{1}{S^2}\left[\left(\frac{\partial S}{\partial v}\right)^2\sigma_v^2 + \left(\frac{\partial S}{\partial r_g}\right)^2\sigma_r^2 + \left(\frac{\partial S}{\partial \rho}\right)^2\sigma_\rho^2 + \sigma_{noise}^2\right] \quad (3)$$

Substituting equation (2) into equation (3), we find that the relationship between the observed dispersion in the signal and random sources of error are:

$$\left(\frac{\sigma_S}{S}\right)^2_{obs} = a^2\left(\frac{\sigma_{r_g}}{r_g}\right)^2 + b^2\left(\frac{\sigma_v}{v}\right)^2 + \left(\frac{\sigma_S}{S}\right)^2_{noise} \quad (4)$$

When used as a detector, the ability to distinguish between two populations of identical projectiles captured at velocities v and $v+\sigma_v$ is fundamentally limited by the detector's intrinsic noise $(\sigma_S/S)_{noise}$.

If we assume that the dispersion we observe in the track signal is entirely due to the intrinsic response of the aerogel detector, then its fractional velocity resolution is given by:

$$\left(\frac{\sigma_v}{v}\right) = \frac{1}{b}\left(\frac{\sigma_S}{S}\right)_{obs.} \quad (5)$$

However, the size distribution of the projectiles and the spread of projectile velocities must be taken into account and their contribution subtracted. The 2, 5, and 20 micron-sized glass bead populations have dispersions in size equal to 35%, 12%, and 10 % respectively (According to the manufacturer, Duke Scientific). The spread of impact velocities is not known for certain, although an experiment that measured the velocity dispersion of a 5 km/s shot showed that this dispersion was on the order of 10 %. If we assume these values for the projectile and impact velocity dispersions of the particles, the velocity dispersion of the detector is given by:

$$\left(\frac{\sigma_v}{v}\right) = \frac{1}{b}\left(\left(\frac{\sigma_S}{S}\right)^2_{obs.} - a^2\left(\frac{\sigma_{r_g}}{r_g}\right)^2 - b^2\left(\frac{\sigma_{v_{obs.}}}{v_{obs.}}\right)\right)^{\frac{1}{2}} \quad (6)$$

Taking these into account gives us a more accurate estimate of the of the velocity resolution of sample 186-2 (Domínguez G. et al. 2004-b)

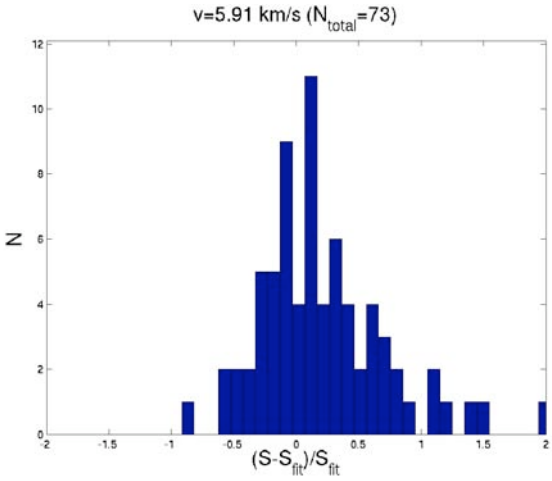

Figure 6. Histogram of the residuals from 5 micron impacts. The residual has been normalized by the value of the best fit to the data, S_{fit}, shown in Fig. 5.

To numerically estimate the velocity resolution of this calorimetric aerogel, we need a measure of the typical dispersion in the observed signal. In Figure 6 we show a histogram of the fractional dispersions of individual 5 micron impacts (v=5.91 km/s). The width of the distribution, $(\sigma_{Sobs.}/S_{obs.}) \sim 0.47$. Using this width, which is typical of the 5 micron data, we conclude that the velocity resolution of calorimetric aerogel sample 186-2 is about 21 %.

4. CONCLUSION

The response function and velocity resolutions of the detector that we have presented here, a SiO2 aerogel doped with Gd (21.3%) and Tb (1.42%) is consistent with the previous results of Domínguez et al. 2003 and Dominguez et al. 2004-b respectively. In particular, it is interesting that the response function parameters *a* and *b* are both close to 2. This suggests that calorimetric aerogels, in general, may respond to the energy-loss of captured projectiles.

Calorimetric aerogels are a promising and attractive technology for studies of natural micrometeorites as well as orbital debris. These aerogels combine the advantages of classical aerogels, i.e. intact capture of hypervelocity particles, particle trajectories, with the advantages of a velocity detector. An added bonus of this technology is that they are completely passive, thus requiring no power while in space.

This instrument that we have presented here represents a significant advance in passive collection technology and could be used, upon retrieval and return to Earth, to characterize both the composition and dynamical properties of orbital debris and natural micrometeorites.

We will incorporate the results of a recent set of experiments (10<v<20 km/s) at the Van de Graaf accelerator at Heidelberg in the near future.

5. ACKNOWLEDGEMENTS

GD, AJW, MLFP, and SMJ were supported by NASA grant NAG5-13284. The work by Giles Graham was performed under the auspices of the US Department of Energy National Nuclear Security Administration by the University of California, Lawrence Livermore National Laboratory under contract No. W-7405-Eng-48.

6. REFERENCES

Anderson W.W. and Ahrens, T.J., Physics of interplanetary dust capture via impact into organic polymer foams, *Journal of Geophysical Research*, Vol. 99(18), 2063–2071, 1994.

Barrett R.A. et al., Suitability of silica aerogel as a capture medium for interplanetary dust, *Proceedings 22nd Lunar and Planetary Science Conference*, 203-212, 1992.

Burchell M.J. et al., Capture of hypervelocity particles in aerogel: in ground laboratory and low earth orbit, *Planetary and Space Science*, Vol. 47, 189–204, 1999.

Borg J. et al., In-situ analyses of Earth orbital grains trapped in aerogel, using synchrotron X-ray microfluorescence techniques, *35th Lunar and Planetary Science Conference*, CD-ROM abstract #1580, 2004.

Domínguez G. et al. (a), Energy loss and impact cratering in aerogels: theory and experiment, *Icarus*, Vol. 172, 613–624, 2004.

Domínguez G. et al. (b), Fluorescent Impact Cavities in a Titatium Doped Al_2O_3-SiO_2 Aerogel: Implications for the Velocity Resolution of Calorimetric Aerogels, *Journal of Non-Crystalline Solids*, Vol. 350C, 385-390, 2004

Domínguez G. et al., A Fluorescent Aerogel for Capture and Identification of Interplanetary and Interstellar Dust, *The Astrophysical Journal*, Vol. 592, 631–635, 2003.

Graham G. A. et al., Mineralogy and microanalysis in the determination of cause of impact damage to spacecraft surfaces, In Pye, K. and Croft, D.J. (eds) *Forensic Geoscience: Principles, Techniques and Applications*, Geological Society, London, Special Publications, 232, 137-146, 2004.

Hörz F. et al., Impact Features and Projectile Residues in Aerogel Exposed on Mir. *Icarus*, Vol. 147, 559–579, 2000.

Johnson N. L. and McKnight D. S., *Artificial Space Debris,* Orbit Book Company, Malabar, Florida, 1991.

Kearsley A.T. et al., Sampling the orbital debris population using a foil residue collector in a standardised container for experiments (SCE), This volume.

Kitazawa Y. et al., Hypervelocity impact experiments on aerogel dust collector, *Journal of Geophysical Research*, Vol. 104, 22035–22052, 1999.

Kitazawa Y. et al., MPAC: Passive measurement experiement of dust particles on ISS, *Proceedings of the 22nd International Symposium on Space Technology and Science*, 2077-2082, 2000.

Maag C.R. and Linder, W.K., Results of space shuttle intact particle experiements, *Hypervelocity Impacts in Space*, Canterbury, 186-190, 1992.

Tillotson T.M. and Hrubesh L.W., Transparent ultralow-density silica aerogels prepared by a 2-step sol-gel process, *Journal of Non-Crystalline Solids*, Vol. 145, 44-50, 1992

Tsou P. Intact capture of hypervelocity projectiles, *International Journal of Impact Engineering* 10, 615-627, 1990.

Westphal A.J. et al., Small hypervelocity particles captured in aerogel collectors: Location, extraction, handling and storage, *Meteoritics and Planetary Science* **37**, 855-865, 2002.

Westphal A.J et al., Aerogel keystones: Extraction of complete hypervelocity impact events from aerogel collectors, *Meteoritics and Planetary Science* Vol. 39, 1375-1386, 2004.